

Gravity currents in a porous medium at an inclined plane

By **DOMINIC VELLA AND HERBERT E. HUPPERT**

Institute of Theoretical Geophysics, Department of Applied Mathematics and Theoretical Physics, University of Cambridge, Wilberforce Road, Cambridge, CB3 0WA, U. K.

(Received 24 May 2019)

We consider the release from a point source of relatively heavy fluid into a porous saturated medium above an impermeable slope. We consider the case where the volume of the resulting gravity current increases with time like t^α and show that for $\alpha < 3$, at short times the current spreads axisymmetrically, with radius $r \sim t^{(\alpha+1)/4}$, while at long times it spreads predominantly downslope. In particular, for long times the downslope position of the current scales like t while the current extends a distance $t^{\alpha/3}$ across the slope. For $\alpha > 3$, this situation is reversed with spreading occurring predominantly downslope for short times. The governing equations admit similarity solutions whose scaling behaviour we determine, with the full similarity form being evaluated by numerical computations of the governing partial differential equation. We find that the results of these analyses are in good quantitative agreement with a series of laboratory experiments. Finally, we briefly discuss the implications of our work for the sequestration of carbon dioxide in aquifers with a sloping, impermeable cap.

1. Introduction

Horizontal differences in density between two fluids lead to the propagation of so-called gravity currents. These currents are of interest in a number of industrial as well as natural applications and so obtaining an understanding of the way in which they propagate is a subject that has motivated a considerable amount of current research (Huppert 2006).

In previous publications, our understanding of axisymmetric viscous gravity currents on an impermeable boundary (Huppert 1982) has been generalised to take account of the effects of a slope (Lister 1992) as well as the propagation of a current in a porous medium (Huppert & Woods 1995; Lyle *et al.* 2005). Here, we consider the propagation of a gravity current from a point source in a porous medium at an impermeable sloping boundary. Of particular interest is the evolution of the current away from the axisymmetric similarity solution found by Lyle *et al.* (2005).

We begin by deriving the evolution equations for the shape of a current whose volume varies in time like qt^α . A scaling analysis of these governing equations reveals the extent of the current as a function of time up to a multiplicative constant. The full form of the similarity solutions that give rise to these scalings can only be determined by numerical means, however, and to do so we modify the numerical code of Lister (1992). For some particular values of α , it is possible to make analytical progress; these cases are considered separately and provide a useful check of the numerical scheme. We then compare the results of the numerical calculations to a series of experiments and find good quantitative agreement between the two. Finally, in the last section, we discuss the implications of our

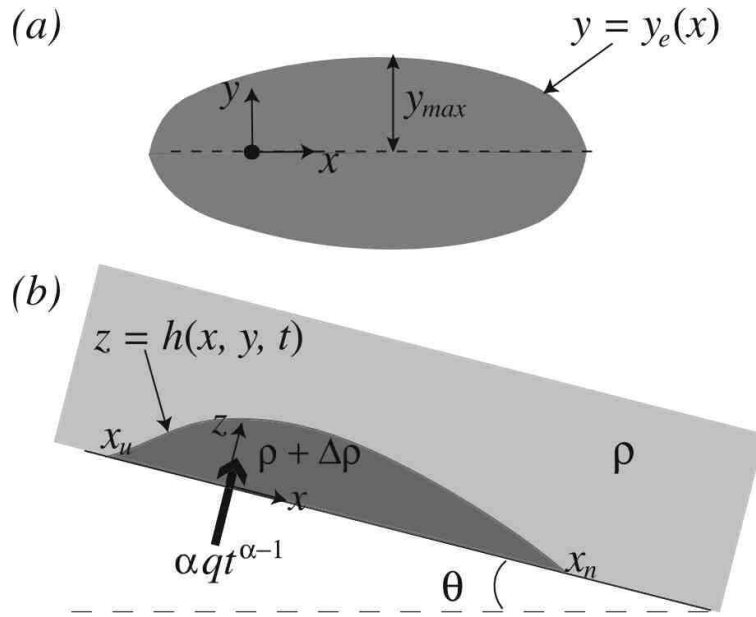


FIGURE 1. Sketches of a gravity current, of density $\rho + \Delta\rho$, propagating in a porous medium saturated with liquid of density ρ above an inclined plane. (a) Plan view of the current and (b) horizontal section through the current.

results in geological settings, with particular emphasis on the implications of our work for the sequestration of carbon dioxide.

2. Formulation

2.1. Governing equations

We consider a gravity current consisting of fluid material of density $\rho + \Delta\rho$ in a deep porous medium saturated with fluid of density ρ , which is bounded by an impermeable barrier at an angle θ to the horizontal (see fig. 1 for a sketch of the setup). That the saturated porous medium is deep in comparison with the vertical extent of the current allows us to neglect the motion of the surrounding fluid, simplifying the problem considerably. We use the natural Cartesian co-ordinate system centred on the mass source and aligned with the slope of the impermeable boundary. The depth, $h(x, y, t)$, of the gravity current is then determined by continuity combined with Darcy's law (see Bear 1988, for example) and the assumption that the pressure in the current is hydrostatic, i.e.

$$P - P_0 = \Delta\rho gh \cos\theta - (\rho + \Delta\rho)gz \cos\theta + \rho gx \sin\theta \quad (z < h), \quad (2.1)$$

with P_0 constant. Using Darcy's law, the velocity within the porous medium is then given by

$$\mathbf{u} = -\frac{k\Delta\rho g}{\mu} \left(-\sin\theta + \cos\theta \frac{\partial h}{\partial x}, \cos\theta \frac{\partial h}{\partial y}, 0 \right), \quad (2.2)$$

where k is the permeability of the porous medium and μ is the viscosity of the liquid. Using this along with the conservation of mass, we obtain

$$\frac{\partial h}{\partial t} = \frac{k\rho g'}{\mu\phi} \left(\frac{\cos\theta}{2} \nabla^2 h^2 - \sin\theta \frac{\partial h}{\partial x} \right), \quad (2.3)$$

where ϕ is the porosity of the porous medium and $g' \equiv g\Delta\rho/\rho$. Equation (2.3) is a nonlinear advection–diffusion equation for the current thickness, with the two terms on the right hand side representing the gravity–driven spreading of the current and its advection downslope, respectively.

It is common to close the system by requiring that the volume of the current depend on time like qt^α for some constant $\alpha \geq 0$ (Huppert 1982; Lister 1992; Huppert & Woods 1995). This constraint leads to solutions of self-similar form (as we shall see again in this case) but also covers the natural cases of a fixed volume release ($\alpha = 0$) and a constant flux release ($\alpha = 1$). To impose this volume constraint, (2.3) must be solved along with

$$\int_{x_u}^{x_n} \int_{-y_e(x)}^{y_e(x)} h \, dy \, dx = qt^\alpha, \quad (2.4)$$

with $|y| = y_e(x)$ giving the edge of the current for $x_u(t) < x < x_n(t)$.

Equations (2.3) and (2.4) may be non-dimensionalised by setting $T = t/t^*$, $H = h/h^*$, $X = x/x^*$ and $Y = y/y^*$, where

$$t^* \equiv \left(\frac{q}{V^3 \tan \theta} \right)^{\frac{1}{3-\alpha}}, \quad x^* = y^* \equiv Vt^*, \quad h^* \equiv x^* \tan \theta, \quad (2.5)$$

and

$$V \equiv \frac{k\rho g' \sin \theta}{\mu\phi} \quad (2.6)$$

is the natural velocity scale in the problem. In non-dimensional terms, therefore, the current satisfies

$$\frac{\partial H}{\partial T} = \nabla \cdot (H \nabla H) - \frac{\partial H}{\partial X}, \quad (2.7)$$

along with the volume conservation constraint

$$\int_{X_u}^{X_n} \int_{-Y_e(X)}^{Y_e(X)} H \, dY \, dX = T^\alpha. \quad (2.8)$$

2.2. *Scalings*

To aid our physical understanding of the spreading of the gravity current, we begin by considering the scaling behaviour of the spreading in the limits of short and long times. This is done by considering the possible dominant balances between the terms in (2.7) and eliminating those that are not self-consistent. For $\alpha < 3$, this analysis reveals that at short times ($T \ll 1$), we observe the axisymmetric scalings obtained by Lyle *et al.* (2005), namely

$$H \sim T^{\frac{\alpha-1}{2}}, \quad X \sim Y \sim T^{\frac{\alpha+1}{4}}. \quad (2.9)$$

Examining the possible balances for $T \gg 1$, we find that, again for $\alpha < 3$, the typical scales of the current vary in time as

$$H \sim T^{\frac{2\alpha-3}{3}}, \quad X \sim T, \quad Y \sim T^{\frac{\alpha}{3}}, \quad (2.10)$$

so that the current spreads predominantly downslope. It is worth noting here that the long time scaling $X \sim T$ is unsurprising because (2.7) may be simplified by moving into a frame moving at unit speed downslope (Huppert & Woods 1995). We also note that the scaling $Y \sim T^{\alpha/3}$ is identical to that found by Lister (1992) for a viscous current on a slope and is in fact generic in these problems, being recovered whenever the fluid flux is proportional to some power of the current height, H .

Regime	Downslope extent	Cross-slope extent	Thickness
$\alpha < 3$	$t \ll t^*$	$\sim \left(\frac{Vq}{\tan \theta}\right)^{1/4} t^{(\alpha+1)/4}$	$\sim \left(\frac{Vq}{\tan \theta}\right)^{1/4} t^{(\alpha+1)/4}$
$\alpha < 3$	$t \gg t^*$	$\sim Vt$	$\sim \left(\frac{q}{\tan \theta}\right)^{1/3} t^{\alpha/3}$
$\alpha > 3$	$t \ll t^*$	$\sim Vt$	$\sim \left(\frac{q}{\tan \theta}\right)^{1/3} t^{\alpha/3}$
$\alpha > 3$	$t \gg t^*$	$\sim \left(\frac{Vq}{\tan \theta}\right)^{1/4} t^{(\alpha+1)/4}$	$\sim \left(\frac{q}{\tan \theta}\right)^{1/4} t^{(\alpha+1)/4}$
			$\sim \left(\frac{q \tan \theta}{V}\right)^{1/2} t^{(\alpha-1)/2}$
			$\sim \left(\frac{q^2 \tan \theta}{V^3}\right)^{1/3} t^{(2\alpha-3)/3}$
			$\sim \left(\frac{q^2 \tan \theta}{V^3}\right)^{1/3} t^{(2\alpha-3)/3}$

TABLE 1. Summary of the asymptotic scalings for the dimensions of a gravity current in a porous medium at an inclined plane. Here dimensional notation is used for clarity, and t^* and V are as defined in (2.5) and (2.6), respectively.

When $\alpha > 3$, the importance of the two downslope terms (the diffusive and translational terms) reverses. In particular, at long times $(HH_X)_X \gg H_X$, so that we in fact recover the axisymmetric spreading scalings given in (2.9) as being relevant for $T \gg 1$. Conversely, for $T \ll 1$ we recover the non-axisymmetric scalings of (2.10). A summary of the different scaling regimes expected is given in dimensional terms in table 1.

That we observe axisymmetric spreading if $\alpha > 3$ and $T \gg 1$ is surprising, but is a consequence of the fact that the downslope flux in a porous medium gravity current is only weakly dependent on the local height and so can be swamped by the spreading terms in (2.7). In the viscous case, this is not possible because the downslope flux is able to remove the incoming flux much more efficiently and penalises the accumulation of material at a particular point more.

2.3. Numerics

The axisymmetric spreading of a gravity current in a porous medium above an horizontal plane was considered by Lyle *et al.* (2005). In particular, they determined the coefficients in the scalings (2.9) by finding a solution dependent on one similarity variable in this case. To determine the prefactors in the non-axisymmetric scaling relations (2.10), it is necessary to resort to numerical solutions of (2.7) and (2.8). The numerical code we used was adapted from that used by Lister (1992) for a viscous gravity current on an inclined plane, with minor alterations to make it applicable to a gravity current in a porous medium. This code is an implementation of a finite-difference scheme on a rectangular grid with time-stepping performed using an alternating-direction-implicit method. Equation (2.7) was written in flux-conservative form allowing the diffusive and advective terms to be represented by the Il'in scheme (Clauser & Kiesner 1987). More details of the numerical scheme may be found in Lister (1992).

3. Special values of α

In this section, we consider separately particular values of α that are of special interest. In some of these cases, it is possible to make progress analytically providing useful checks on the numerical scheme discussed in §2.3, but they also shed light on situations of practical interest.

3.1. Constant volume

As already noted, the differential equation in (2.7) may be simplified by moving into a frame translating at unit speed downslope. However, for general values of α , this corresponds to a point source that is moving uphill in the new frame, complicating the

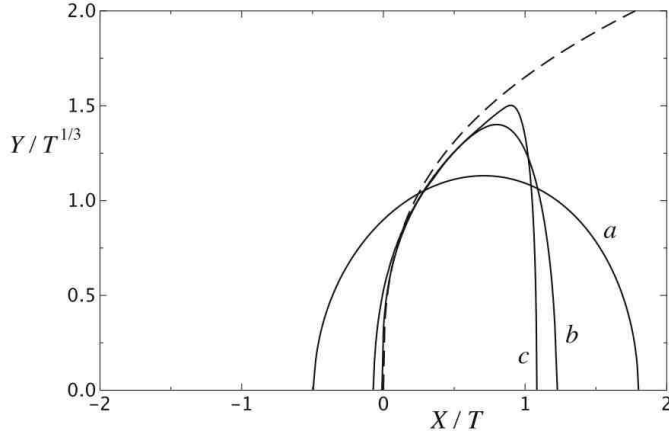


FIGURE 2. Numerical evolution of the boundary of the current in rescaled co-ordinates at (a) $T = 1.23$, (b) $T = 9.52$ and (c) $T = 270.9$. The last of these is indistinguishable from the steady state shape that is found at long times in these rescaled variables. The similarity solution for the steady shape in the interior is given by $Y = (9X/2)^{1/3}$ (dashed line) and is valid away from the source and the front regions, which in these rescaled variables requires that $T^{-1} \ll X/T \ll 1$.

analysis. For a current of constant volume, $\alpha = 0$, there is no distinguished source point and we let $X' \equiv X - T$. The resulting transformation of (2.7) has an axisymmetric similarity solution (Lyle *et al.* 2005), which may be written

$$H(X, Y, T) = \frac{1}{8T^{1/2}} \left(\frac{4}{\sqrt{\pi}} - \frac{R'^2}{T^{1/2}} \right), \quad (3.1)$$

where $R' \equiv (X'^2 + Y^2)^{1/2}$.

3.2. Constant flux: A steady state

For very long times $T \gg 1$, we expect that a constant flux current (corresponding to $\alpha = 1$) will approach a steady state, whose shape we now determine. We expect this steady shape to be observed far from the nose of the current, since the nose is always unsteady, requiring that $X \ll T$. Sufficiently far downstream from the source ($X \gg 1$), the steady shape is given by

$$\frac{\partial^2 H^2}{\partial Y^2} = 2 \frac{\partial H}{\partial X}, \quad (3.2)$$

which has a similarity solution of the form $H(X, Y) = X^{-1/3}f(Y/X^{1/3})$ where the function f satisfies

$$\frac{d^2 f^2}{d\eta^2} + \frac{2}{3} \left(f + \eta \frac{df}{d\eta} \right) = 0, \quad \int_{-\eta_e}^{\eta_e} f d\eta = 1, \quad f(\pm\eta_e) = 0. \quad (3.3)$$

This has solution

$$f(\eta) = \frac{1}{6}(\eta_e^2 - \eta^2), \quad (3.4)$$

where $\eta_e = (9/2)^{1/3} \approx 1.651$ denotes the position of the current edge in similarity variables.

This shows that far away from the source and nose regions, we should expect the shape of unsteady currents to approach $Y = (9X/2)^{1/3}$. Superimposing this curve onto the

numerically calculated current provides a useful check of the numerical scheme described in §2.3. This comparison (see fig. 2) shows that, away from both the nose and source regions, we do indeed see the steady state shape, though this region is confined to $T^{-1} \ll X/T \ll 1$ in the rescaled co-ordinates used in fig. 2.

It is interesting to note that the similarity solution (3.4) is precisely that given by Huppert & Woods (1995) for the shape of a two-dimensional current of constant volume spreading in a porous medium above an horizontal boundary. This correspondence arises because in the steady state case considered here, fluid moves downslope at a constant velocity — independently of its cross-slope position and the current height — so that X is a proxy for time. A material slice in the y - z plane thus remains planar as it is advected downslope and so spreads laterally in exactly the same way that a fixed volume release does in two-dimensions.

3.3. $\alpha = 3$

When $\alpha = 3$, the non-dimensionalisation leading to (2.7) breaks down because there is no longer a characteristic time-scale t^* of the motion. Instead, an additional natural velocity scale, $q^{1/3}$, enters the problem. We thus define a new set of dimensionless variables $\tilde{T} = t/t^*$, $\tilde{H} = h/\tilde{h}^*$, $\tilde{X} = x/\tilde{x}^*$ and $\tilde{Y} = y/\tilde{y}^*$ where \tilde{t}^* is an arbitrary timescale and

$$\tilde{x}^* = \tilde{y}^* \equiv \left(\frac{q}{\tan \theta} \right)^{1/3} \tilde{t}^*, \quad \tilde{h}^* \equiv \tilde{x}^* \tan \theta. \quad (3.5)$$

In these non-dimensional variables, the system becomes

$$\frac{\partial \tilde{H}}{\partial \tilde{T}} = \delta \left(\nabla \cdot (\tilde{H} \nabla \tilde{H}) - \frac{\partial \tilde{H}}{\partial \tilde{X}} \right), \quad (3.6)$$

along with volume conservation in the form

$$\int_{\tilde{X}_u}^{\tilde{X}_n} \int_{-\tilde{Y}_e(\tilde{X})}^{\tilde{Y}_e(\tilde{X})} \tilde{H} d\tilde{Y} d\tilde{X} = \tilde{T}^3, \quad (3.7)$$

where $\delta \equiv V(\tan \theta/q)^{1/3}$ is essentially the ratio of the two velocity scales in the problem. By substituting $\tilde{H} = \tilde{T}\phi(\xi, \eta)$ with $\tilde{X} = \tilde{T}\xi$ and $\tilde{Y} = \tilde{T}\eta$, time can be eliminated from this problem completely so that ϕ is the solution of the two-dimensional problem

$$3\phi = [\phi(\xi + \delta(\phi_\xi - 1))]_\xi + [\phi(\delta\phi_\eta + \eta)]_\eta, \quad (3.8)$$

(with subscripts denoting differentiation) and

$$\int_{\xi_u}^{\xi_n} \int_{-\eta_e}^{\eta_e} \phi d\eta d\xi = 1. \quad (3.9)$$

The system (3.8) and (3.9) was solved by timestepping the problem in (3.6) and (3.7) using a minor modification of the code described in §2.3. This was found to be a convenient method of solution and also demonstrates that time-dependent solutions converge on the time-independent solution. The results of this calculation are shown in fig. 3 for a number of different values of δ .

The importance of the case $\alpha = 3$ as a transition between qualitatively different flow regimes is reminiscent of earlier work on gravity currents. For an axisymmetric gravity current, Huppert (1982) found that viscous forces dominate inertia at long times for $\alpha < 3$ (being insignificant at short times) with the situation reversed for $\alpha > 3$. Acton *et al.* (2001) found that a viscous gravity current propagating over a permeable medium spreads

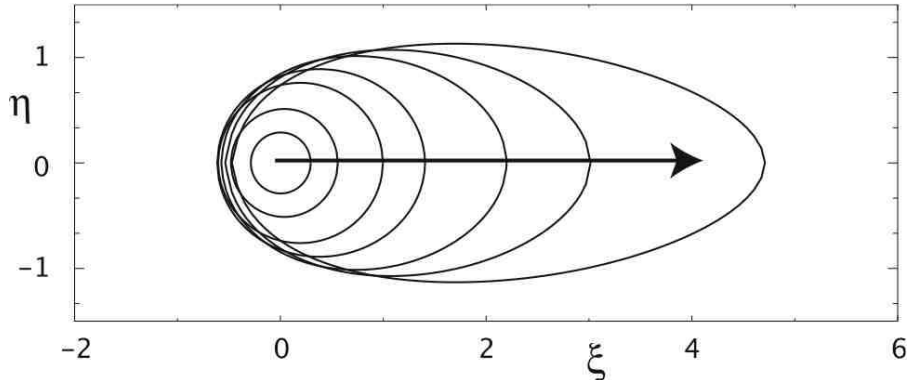


FIGURE 3. Numerical results showing the shape of currents with $\alpha = 3$ obtained by solving (3.8) and (3.9) for various values of the parameter δ . Here the arrow indicates the direction of increasing δ , with current shapes shown for $\delta = 0.01, 0.1, 0.5, 1, 2, 3$ and $\delta = 5$.

only a finite distance if $\alpha < 3$ but spreads indefinitely for $\alpha > 3$. Despite these similarities, the reappearance of a transition at $\alpha = 3$ here is purely coincidental.

3.4. $\alpha > 3$

In §2.2, we observed that for $\alpha > 3$ a scaling analysis suggests that we should observe axisymmetric spreading for $T \gg 1$. For such values of α , therefore, we expect to recover the axisymmetric solutions given by Lyle *et al.* (2005) in our numerical simulations. In particular, for $\alpha = 4$ we would expect to find that

$$X_n, Y_{\max} \sim 0.8855T^{5/4},$$

where the prefactor here has been determined from the analysis of Lyle *et al.* (2005). As shown in fig. 4, this result is indeed obtained from our numerical results.

4. Experimental results

We conducted experiments in which a saline solution (dyed red) was injected at constant flux ($\alpha = 1$) into the base of a porous medium saturated with fresh water. The details of the experimental setup are as described by Lyle *et al.* (2005) although the perspex tank was tilted (so that the gravity current was propagating on a slope). Additionally, the saline solution was injected at the edge of the tank, away from the corner because the inherent symmetry is different here to that of the axisymmetric case. Video footage of the motion was captured using a CCD camera and measurements of the front distance down slope x_n as well as the maximum lateral extent of the current y_{\max} were made using the image analysis software ImageJ†. The details of the six different values of g' , q and θ investigated are given in table 2, along with the relevant values of the typical scales t^* , x^* and h^* . The latter estimates are based on the measurements of $\phi = 0.37$ and $k = 6.8 \times 10^{-9} \text{ m}^2$ given by Lyle *et al.* (2005).

The experimental results plotted in fig. 5 shows that the experimental results are in good agreement with the theoretical results produced by solving (2.7). In particular, the scalings predicted in (2.10) are borne out by these results although the associated prefactors are only correct to within $\sim 20\%$. This is a similar level of disagreement to

† ImageJ is distributed by the National Institutes of Health and may be downloaded from: <http://rsb.info.nih.gov/ij/>

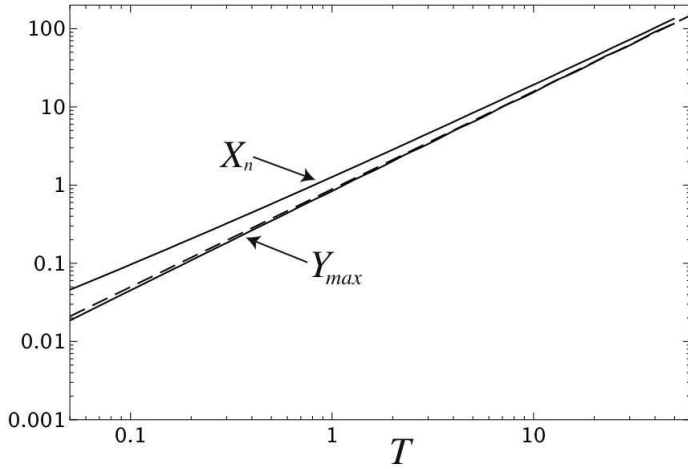


FIGURE 4. Numerical results for the positions of the current edge X_n and Y_{max} as a function of time T for $\alpha = 4$ (solid lines). For $T \gg 1$ these obey the axisymmetric spreading relationship, $X_n, Y_{max} \sim 0.8855T^{5/4}$ (dashed line), that we expect from the axisymmetric analysis of Lyle *et al.* (2005).

Expt.	Symbol	g' (cm s ⁻²)	q (cm ³ s ⁻¹)	θ (°)	t^* (s)	x^* (m)	h^* (m)
1	△	91	2.14	9.5	24.5	0.068	0.011
2	□	99	1.31	10	15.4	0.049	0.009
3	◇	99	3.04	18	7.3	0.041	0.013
4	●	99	4	18	8.3	0.047	0.016
5	■	99	5.78	18	10	0.056	0.018
6	★	91	3.86	5	118.9	0.174	0.015

TABLE 2. Parameter values investigated in the six experiments presented here as well as the symbol used to represent their results in fig. 5.

that found by Lyle *et al.* (2005). Two possible mechanisms may account for this discrepancy: mechanical dispersion of the intruding saline solution (see Brady & Koch 1988, for example) and the fact that the pore Reynolds number in our experiments is typically $O(5)$. Such a value of the pore Reynolds number suggests that we may be approaching the regime where Darcy's law begins to break down, which is around $Re = 10$ (Bear 1988). Neither of these mechanisms, however, seem to account for the observation that the downslope extent of the current, X_n is systematically below that predicted, while the cross-slope spreading observed is more than that predicted.

5. Geological relevance

Our experimental and numerical analyses have shown that shortly after the initiation of a constant flux gravity current ($\alpha = 1$) it begins to spread axisymmetrically in the manner described by Lyle *et al.* (2005). However, at times much longer than the characteristic time t^* given in (2.5), the current loses its axisymmetry and propagates predominantly downslope. Since it propagates at constant velocity in this regime, the

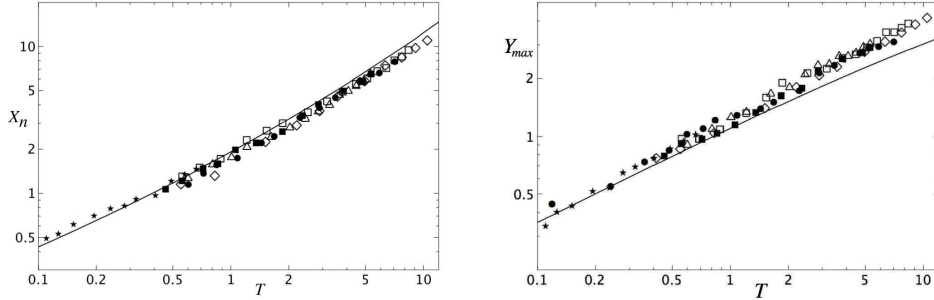


FIGURE 5. Numerical (solid line) and experimental (points) results for the position of the nose of the current, X_n , and the maximum horizontal extent of the current, Y_{\max} , as functions of time. The symbols used to represent each experimental run are given in table 2.

current propagates much further and faster in this case than would be the case if it remained axisymmetric. This is potentially problematic in a range of practical applications, such as the sequestration of carbon dioxide in which super-critical carbon dioxide is pumped into aquifers. Since the density of the liquid carbon dioxide lies in the range $500 \pm 150 \text{ kgm}^{-3}$ (Chadwick *et al.* 2005), it remains buoyant with respect to the ambient water and so will rise up any inclined boundaries.

The time-scale, t^* , over which asymmetric spreading develops is of interest to those wishing to predict the course of the released current. While it is difficult to evaluate t^* in a precise manner because of the uncertainties in the properties of the surrounding rock, we can perform some estimates on the basis of the available data from the Sleipner field (Bickle *et al.* 2005; Chadwick *et al.* 2005). In this Norwegian field, around 10^9 kg of liquid CO_2 is currently pumped into the local sandstone each year. Presumably due to geological complications, this single input flux is observed later to separate into around ten independent currents propagating within different horizons of the permeable layer, each of which has a volume flux lying in the region $0.002 \lesssim q \lesssim 0.03 \text{ m}^3\text{s}^{-1}$. Combined with typical measured values for the porosity and permeability of $0.7 \leq k \leq 5 \times 10^{-12} \text{ m}^2$ and $\phi = 0.31 \pm 0.04$ as well as the CO_2 viscosity, $\mu = 3.5 \pm 0.5 \times 10^{-5} \text{ Pas}$ (Bickle *et al.* 2005) we can estimate upper and lower bounds on the value of t^* . When $\theta = 1^\circ$, we find that $0.02 \leq t^* \leq 7.4$ years. This suggests that the effects of non-axisymmetric spreading may indeed be important and may also be observable in the field. Because of the variety of values of the slope that we might expect to encounter in any geological setting, we note also that for $\theta \ll 1$, $t^* \sim \theta^{-4/(3-\alpha)}$. For constant pumping rate ($\alpha = 1$), this gives $t^* \sim \theta^{-2}$; i.e. the precise value of the timescale over which the current becomes asymmetric depends sensitively on θ . This suggests that the different spreading regimes discussed here may be observed in the field and may also have practical implications.

Since injection occurs into confined layers of sediment, estimates for the vertical scale of the current, h^* , are also important. Interestingly, h^* is independent of θ for $\theta \ll 1$ (measured in radians) and $\alpha = 1$ so that, with the parameter values given above, we find $0.7 \leq h^* \leq 13 \text{ m}$. This suggests that, near the source, the depth of the sediment layer may be similar to that of the current (and so exchange, confined flows may become significant). However, we expect that the scaling $H \sim T^{-1/3}$ valid away from the source ensures that the present study will remain valid downstream.

We are grateful to John Lister for access to his code for a viscous current on a slope and to Robert Whittaker for discussions. Mike Bickle, Andy Chadwick, Paul Linden and John Lister also provided valuable feedback on an earlier draft of this paper.

REFERENCES

- ACTON, J. M., HUPPERT, H. E. & WORSTER, M. G. 2001 Two-dimensional viscous gravity currents flowing over a deep porous medium. *J. Fluid Mech.* **440**, 359–380.
- BEAR, J. 1988 *Dynamics of Fluids in Porous Media*. Dover.
- BICKLE, M., CHADWICK, A., HUPPERT, H. E., HALLWORTH, M. A. & LYLE, S. 2005 Modelling carbon-dioxide accumulation in the sleipner field: Implications for carbon sequestration (in preparation).
- BRADY, J. F. & KOCH, D. L. 1988 Dispersion in porous media. In *Disorder and Mixing* (ed. E. Guyon, J.-P. Nadal & Y. Pomeau), pp. 107–122. Kluwer.
- CHADWICK, R. A., ARTS, R. & EIKEN, O. 2005 4D seismic imaging of a CO₂ plume. In *Petroleum Geology: North-West Europe and Global Perspectives—Proceedings of the 6th Petroleum Geology Conference* (ed. A. G. Doré & B. A. Vining), pp. 1385–1399. The Geological Society, London.
- CLAUSER, C. & KIESNER, S. 1987 A conservative, unconditionally stable, second-order, three-point differencing scheme for the diffusion-convection equation. *Geophys. J. R. Astr. Soc.* **91**, 557–568.
- HUPPERT, H. E. 1982 The propagation of two-dimensional and axisymmetric viscous gravity currents over a rigid horizontal surface. *J. Fluid Mech.* **121**, 43–58.
- HUPPERT, H. E. 2006 Gravity currents: A personal perspective. *J. Fluid Mech.* (in press).
- HUPPERT, H. E. & WOODS, A. W. 1995 Gravity-driven flows in porous layers. *J. Fluid Mech.* **292**, 55–69.
- LISTER, J. R. 1992 Viscous flows down an inclined plane from point and line sources. *J. Fluid Mech.* **242**, 631–653.
- LYLE, S., HUPPERT, H. E., HALLWORTH, M. A., BICKLE, M. & CHADWICK, A. 2005 Axisymmetric gravity currents in a porous medium. *J. Fluid Mech.* **543**, 293–302.